



Transmission of and fouling by long chain molecules during crossflow microfiltration of algal suspensions: influence of shear

Pharima Pongpairoj^{a,*}, Robert Field^a, Zhanfeng Cui^a, Filicia Wicaksana^b, Anthony G. Fane^b

^aUniversity of Oxford, Department of Engineering Science, United Kingdom
Tel. + 44 01865 273190; email: pharima.pongpairoj@eng.ox.ac.uk

^bNanyang Technological University, Singapore Membrane Technology Centre, Singapore

Received 10 February 2011; Accepted 17 May 2011

ABSTRACT

Fouling is the main obstacle in membrane filtration, especially in the water industries. Membrane fouling by algae and its secreted extracellular polysaccharide is still an ongoing problem. Flux stepping microfiltration experiments of *Chlorella Sorokiniana* were carried out using Direct Observation Through Membrane (DOTM) equipment. The trend of extracellular polysaccharide (EPS) transmission during micro-filtration of *Chlorella Sorokiniana* was found to be dependent on flux as well as crossflow velocity (CFV). Increases in flux during flux stepping experiments generally resulted in an initial increase in transmission of EPS through the membrane. Further increases in flux, however led to unexpected results. At low crossflow velocity, EPS transmission did not vary significantly with flux. At higher crossflow velocity, EPS transmission initially increased as flux increased however the transmission then reduced as flux was increased to higher values. Interestingly, EPS concentration in the permeate was much higher than that of the feed supernatant at higher crossflow velocities. This implies that $C_p > C_b$, or negative retention, therefore the effect of concentration polarisation alone of solutes in the supernatant cannot be used to explain this phenomena. Furthermore EPS transmission through Anopore membranes was unexpectedly higher for the 0.1 μm membrane than for the 0.2 μm membrane. PVDF, with its broader pore size distribution and interconnected pores, resulted in greater amounts of EPS transmission than Anopore membranes of the same 0.2 μm pore size. These phenomena could result from the changes in the structure and composition of the concentration polarization layer especially near the pore entrances and from shear within the system which may act to remove some of the gelatinous sheath around the cells. The effects due to shear within the system are highlighted here. In order to relate the effect of shear and basic polymeric transport to EPS transmission through membrane pores, a brief review of transport of a polymer through a pore is presented. From this a rationalisation of observations on the deposition and removal mechanisms of algal cells (a physical model of interaction of algae and EPS with the membrane) as seen using DOTM is proposed.

Keywords: Microalgae; Fouling; Transmission; Shear; Filtration; Polysaccharide

*Corresponding author.

1. Introduction

Membrane technology is very attractive in today's world as it often offers not only a potentially more economic but also an environmental friendly solution compared to more established technologies. Membrane usage is particularly important in the water industries. However fouling and cleaning of membranes is still an important issue. The presence of algae in natural water is a major obstacle in membrane operations as it results in an increase in transmembrane pressure (TMP) or a decrease in flux (J) [1]. In desalination processes, fouling of microfiltration and ultrafiltration membranes during seawater pretreatment is more pronounced during algae bloom [2]. In some cases, after an algae bloom, it is necessary for the membranes to be taken off-line and cleaned [2]. The deposition of algal cells on the membrane surface results in an increase in operating costs [1]. Many studies of algal filtration have been made, but their fouling mechanism has not been well understood. Understanding the nature and characteristics of the algae is crucial as this is the key to the interpretation of the results.

The algae used here are fresh water algae, *Chlorella Sorokiniana*, as it is one of the genus that represents green algae which are commonly found in natural water [3]. Similar to many other macromolecules, they secrete extracellular polysaccharides (EPS). Members of the *Chlorella* genus usually inhabit a hydrosphere. The hydrosphere around the algal cells is also known as the sheath, it is believed that the substance is produced in order to aid symbiotic association as well as absorption of metal ions. Generally, the sheath produced in microalgae leads to aggregation of cells in aquatic systems [4]. It provides an intermediate role for communication of cells in symbiotic association which promotes algal growth by creating a suitable habitat [4–6]. For *Chlorella Sorokiniana* IAM C212, a polysaccharide gel is produced as a sheath under photoautotrophic conditions. *Chlorella Sorokiniana* was seen to have both adherence to its symbionts and were bound together through the sheath produced [7]. The sheath of *Chlorella Sorokiniana* consisted of a metal and algal photosynthate [4]. Although some information regarding the symbiotic association is available, symbionts of *Chlorella* as well as relationships between microalgal sheath and symbiosis are not clearly identified.

The composition of the mucilage sheath or extracellular polymeric saccharide has been found to consist of a variation of saccharides generated as photosynthetic metabolites, divalent cations contained in the culture medium, as well as proteins, lipids and inorganic ash [4]. A picture of the sheath matrix produced by *Chlorella Sorokiniana* is shown in Fig. 1. The EPS characteristic and productivity are affected

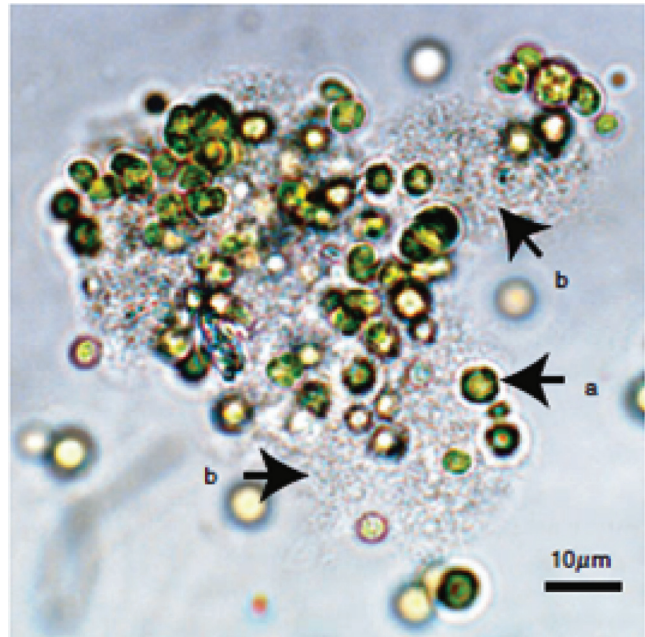


Fig. 1. Sheath matrix produced by *Chlorella Sorokiniana* IAM-212 (a) *C. Sorokiniana* (b) sheath. Reproduced with permission [6].

by metal cations [4]. *Chlorella Sorokiniana* sheath can be increased by introduction of calcium chloride solution which results in coflocculation of the algae and the associated symbiotic bacteria [4]. The precipitation/sedimentation of gelatinous saccharides was found to increase as the concentration of calcium and strontium chlorides increased. However with addition of NaCl, KCl, or $MgCl_2$, no saccharide precipitation was observed even though Mg^{2+} is the major metal ion component in the sheath. This may be “due to differences in the affinity between the secreted saccharide and the metal ions [4]”. Alginate gelation was influenced differently by different types of metal ions. The amount of sheath produced increased, and the cells were flocculated in the gelatinous sheath. The saccharide concentration in the broth decreased, but this decrease is equivalent to the quantity of gelled saccharides adhering to the algal cells [4].

It has been hypothesised that amelioration of fouling can be achieved through the use of operations and transient shear for example crossflow velocity and air-sparging. Nevertheless for some cases such as MBRs, it has been reported that too large a crossflow velocity and/or too higher an aeration rate can lead to higher overall resistances and a greater portion of irreversible fouling [8]. For algae filtration, it is known that the EPS secreted is responsible for severe membrane fouling. The specific cake resistance of membranes in *Chlorella* algae filtration has

been found to relate directly to the amount of extracellular organic matter within the feed [9]. Moreover, Babel et al. found that the developed cake resistance did not vary with the membrane materials used [10]. Chiou et al. compared filtration of 3 algae species, and the species which has the highest amount of EPS fouled the membranes most severely [11]. There are a few studies on shear and algae filtration. Crossflow filtration was believed to result in better performance than dead end filtration [12]. The effect of shear on the feed stock prior to algae microfiltration and ultrafiltration have also been observed [2]. As expected, pre-shear samples with higher EPS substances led to higher membrane fouling [2]. Several algae fouling mitigation techniques have been used, these include coagulation and preozonation [13]. Nevertheless, the formation of a more compact cake as a result of the coagulants may lead to a higher fouling rate as found in bacterial floc microfiltration [14].

Greater understanding of the foulant behaviour is required for fouling mitigation. The use of direct observation through membrane (DOTM) system, allows a non-invasive optical observation of the foulant on the membrane surface. The optical images were used together with TMP to observe membrane fouling of *Chlorella Sorokiniana*. Understanding the transmission of polysaccharides by the membranes is of importance in many applications including desalination and MBR operations. A brief review of transport of polymer through pore and a rationalisation of visual observation are included with this paper as they help explaining the fouling phenomena.

2. Experimental (materials and methods)

2.1. Feed

Pure culture of *Chlorella Sorokiniana* was obtained from American Type Culture Collection (ATCC). The algae were cultured in photoautotrophic condition at room temperature in a photobioreactor of 3 l working volume. During cultivation, a mixture of carbon dioxide gas and air of volume ratio 3:100 was introduced into the system to maintain optimal growth. Harvesting of the algae was done at approximately 14 days where algal concentration is at its maximum. Upon harvesting, concentration was found to be approximately 2 g dry weight/l. Dry weight together with calibration curves relating algae concentration-UV absorbance was carried out. UV spectrophotometer (UV-1800, Shimadzu UV Spectrophotometer) was set to measure the absorbance at various wavelengths. Measurements at 490 nm were used for analysis. Diluted algal mixtures were then used as feed to the filtration cell.

2.2. Crossflow membrane filtration unit

A schematic drawing of the DOTM filtration process is shown in Fig. 2. The DOTM cross-flow filtration cell consists of a conventional crossflow cell that is made of Perspex with a glass viewing window. An optical microscope, Axiolab, Zeiss, was used to focus through the back of the membrane, and images of the membrane skin on the feed side were periodically captured by colour video camera, JVC, TK-C921BEG. These images were captured using Image pro plus software, and the same software was used for image analysis. Magnification of 10x was found to produce clear images for image analysis. The transparent membranes used for image analysis experiments were Anopore flat sheet membrane from Whatman. This setup is a modified version of the DOTM set up used by Li et al. [15].

The setting of the crossflow filtration cell is upside down so that settling of the feed material on to the membrane due to gravity is avoided. The inlet, outlet, and the permeate were connected with identical pressure transducers (Model 206, Cole Palmer). Crossflow velocity was generated by a gear pump (Gear pump drive, Cole Palmer). A peristaltic pump (Minipuls3, Gilson) was connected at the permeate side to control flux. An electronic balance (Model PL4002, Mettler Toledo) was used to measure the permeate. These data are feed to a PC via a datalogging system using Labview software. The feed was continuously stirred at 500 rpm by a magnetic stirrer bar with magnetic coupling generated by a Barnstead Cimarec Digital Hot Plate Stirrer (Barnstead/Thermolyne).

Deionised water was used throughout, and was prepared by a MilliQ system with 0.22 μm Millipak express. Prior to starting each experiment, the system was flushed thoroughly with deionised water for at least half an hour.

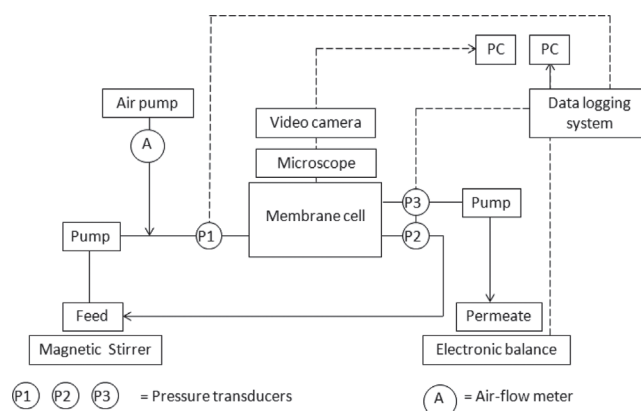


Fig. 2. Schematic drawing of DOTM.

For each experiment, a new membrane sheet was used, and its initial water permeability was measured. All experiments operated using recirculation. For analysis of Organic content, a small sample was collected from the feed tank at the beginning and the end of each flux stepping. The permeate was also collected separately for each 17.5 min period. Flux-Transmembrane pressure measurements were recorded every 10 s.

2.3. The membrane

Anopore 0.2 μm , 0.1 μm and PVDF 0.2 μm membranes were used in these experiments. Anopore is a aluminium oxide membrane with precise, non-deformable, highly controlled, uniform capillary structure ‘with no lateral crossovers between individual pores’ [16,17]. The contact angles of Anopore and PVDF membranes measured using the sessile drop technique (DataPhysics OCA-series) are 9.5–10.2° and 28–30° respectively. The pore size distribution of the Anopore membrane is narrow, whilst the PVDF membrane showed a broad distribution. This was done using (CFP-1500A, Porous Materials, Inc.) [18].

2.3.1. Membrane sheet preparation

Each membrane is mounted between 150 gsm A4 paper. Holes are cut in the paper and the circular disk is glued between two sheets; the glue also prevents water penetration. This approach accommodates a circular disk in a rectangular cell and also provides the membrane area with stable flow and minimizes entrance effects which would otherwise give rise to unstable flow. The arrangement is the typical technique used for DOTM [15]. Blank test membrane sheets (without membrane) were tested to confirm that the surface was not permeable to water or damaged by the flow even at the highest crossflow velocity used for the experiments for the limited time used. The membrane sheet was also tested by soaking in water overnight as well as testing it rigorously in the test cell.

This system appeared to work well although for long term experiments and at high crossflow velocity, an indentation became visible near the feed inlet of the membrane sheet. However, because the distance between the Anopore membrane and this indentation was large, the effect on membrane filtration was considered minimal.

2.4. Suspension analysis

An UV spectrophotometer (UV-1800, Shimadzu UV Spectrophotometer) was used to relate algae concentration to UV absorbance. A linear relationship between

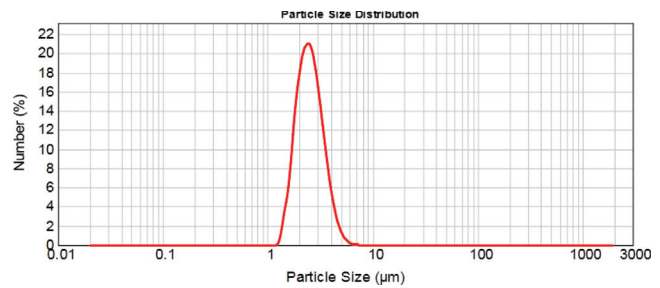


Fig. 3. Particle size distribution of *Chlorella Sorokiniana* measured using Mastersizer 2000.

these occurred for the dilution range used for the experiments. Algae concentration of the feed tank was measured every 17.5 min via the above method. As the membrane pore sizes of 0.2 and 0.1 μm are much smaller than the size of the algae (around 3 μm), none of the algal cells were presented on the permeate side. At the dilutions used in the experiments the viscosity of the algae solution did not deviate noticeably from that of water.

Particle size distribution was measured using Particle analyzer (Mastersizer 2000, Malvern, UK). Fig. 3 shows particle size distribution (as number %) of algae diluted with deionised water.

2.4.1. Measurement of extracellular polysaccharide and organic content

The feed samples were concentrated by refrigerated centrifuge (Sorvall Legend Mach 1.6R, Thermo scientific) at 4000 rpm at 4°C for 10 min. The fluid was removed and labelled as supernatant. The pellet remaining was extracted via a chemical method. 0.6 ml of 8.5 wt.% NaCl and 0.22 wt.% formaldehyde solution and 4.4 ml of deionised water were added to 10 ml samples and this mixture was incubated at 4°C for one hour. After that 0.4 ml of 1.0 M NaOH and 4.6 ml of deionised water were added. A further incubation period of 3 h was required. After the extraction procedure had been completed, the solution was transferred to 2 ml centrifuge tubes and was centrifuged at 13200 rpm at 4°C for 20 min (CT15E Series, Hitachi Koki Co. Ltd). The extracted liquid was labelled as pellet extractant.

Supernatant, extraction from the pellets, as well as the permeate sample of each flux step were then analysed using the following methods.

2.4.2. Colorimetric determination of polysaccharide concentration (EPS-Polysaccharide)

Measurements of Polysaccharides of the collected samples were analysed using the Sulphuric-Phenol method (Dubois method). This was done by addition

of 1 ml 5 wt.% phenol solution and 5 ml of concentrated sulphuric acid (H₂SO₄) to 2 ml of analyte and mix well. After 10 min of reaction time, UV absorbance of the analyte was carried out at 492 nm. The UV absorbance was found to be proportional to the total carbohydrate concentration within the solution (Glucose equivalent).

2.4.3. Colorimetric determination of protein concentration (EPS-Protein)

BCA Protein assay kit for protein assay using Bicinchoninic acid (Product number 23225, Thermo Scientific) was used. BCA Protein assay Reagent A was used together with BCA Protein assay Reagent B, at A:B ratio of 50:1. The solution was added into the supernatant, the pellets extractant and the permeate sample at a ratio of 20 to 1 (2 ml of BCA working solution per 0.1 ml of analyte). These solutions were incubated at room temperature for exactly 120 min then UV absorbance was measured at 562 nm by UV spectrophotometer (UV-1800, Shimadzu UV Spectrophotometer). The UV absorbance relates to the concentration of proteins within the solution (BSA equivalent).

2.4.4. Measurement of total organic carbon

Measurement of total organic carbon (TOC) of the supernatant solutions and the permeate samples from each flux step were carried out using Total organic carbon analyser (TOC-V CSH, Shimadzu). Prior to the measurement, each sample was filtered through a 0.45 µm syringe filter (Acrodisc syringe filter, Pall) to assure that particle size within the solution was below the machine's threshold limit.

2.5. Analysis of transmembrane pressure

Due to a large amount of noise in the data, and for additional accuracy of data analysis, a different approach to the conventional way used in membrane filtration was employed. A signal processing technique, the Savitzky-Golay filter smoothing method (OriginLab), was used to remove noise from the raw data signal. Savitzky-Golay is a polynomial regression which reveals the data smoothed values while the peak height and width is preserved [19]. Transmembrane pressure flux curves were shifted to the same starting point. From the TMP-J data average transmembrane pressure and average flux for each flux step were plotted. Rate of increase of transmembrane pressure was then revealed. In this way, the overview of transmembrane pressure and the rise in transmembrane pressure at each flux step for various systems can be easily compared.

3. Results and discussion

Flux-stepping crossflow filtration of *Chlorella Sorokiniana* was carried out at subcritical and supercritical flux of the algal cells. TMP-J data was used together with DOTM image analysis to reveal algal depositions on the membrane surface. Crossflow velocities were set at three levels 0.107, 0.175, and 0.237 m/s. Higher crossflow velocities lead to lower algal deposition on the membrane surface for both subcritical and supercritical flux experiments. However for subcritical flux experiments, the TMP were higher at higher crossflow velocities than at lower crossflow velocities. Further experiments were then carried out to observe this with EPS and TOC of the feed and the permeate being monitored throughout. The effect of membrane pore size and membrane type on EPS transmission was also observed and discussed in this paper.

3.1. Effect of crossflow velocity

3.1.1. TMP trends and coverage results

Experiments were carried out to observe the behaviour of algae at supercritical fluxes of the algae. As expected, higher crossflow velocity lead to higher removal of algal cells and resulted in less deposition of algal cells on the membrane. As shown in Fig. 4, the deviation of average transmembrane pressure against flux from that of the clean water values was less significant at high crossflow velocity. This result is supported by DOTM images; higher crossflow velocities resulted in slower and less deposition of the algal cells on the membrane surface compared with that at lower crossflow velocity. For crossflow operation, it is believed that

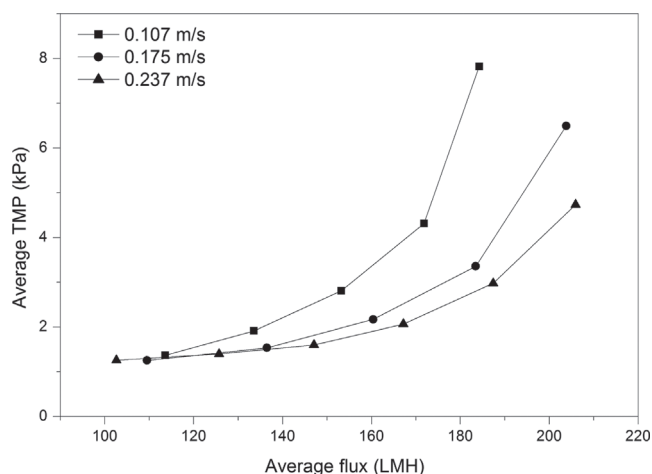


Fig. 4. Transmembrane pressure against flux for 29 mg/l algae solution at different crossflow velocities when flux stepping started from above the critical flux of the algal cells.

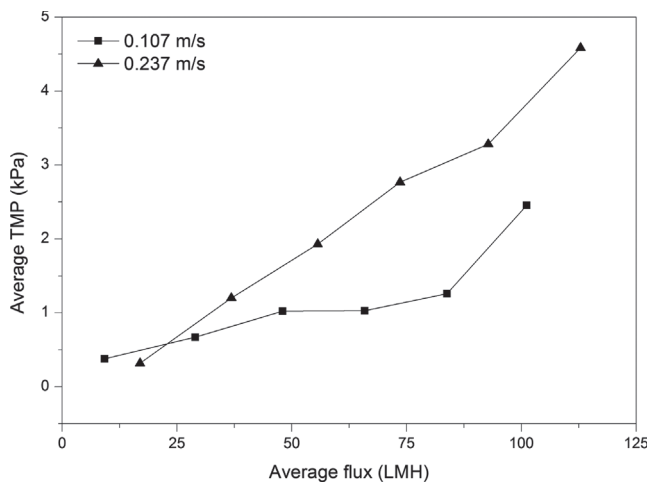


Fig. 5. Transmembrane pressure against flux for 29 mg/l algae solution at different crossflow velocities when flux stepping started from below critical flux for the algal cells.

the effect of shear induced diffusion reduces deposition of the solutes as shear increases and this was observed with the use of DOTM.

However when the starting flux of the flux stepping was reduced to a subcritical level, an opposite effect of crossflow velocity was found as shown in Fig. 5). Surprisingly, the TMP is higher at a given flux for the higher CFV. Interestingly the deviation of average transmembrane pressure against flux from clean water values was less at low the crossflow velocity. For low crossflow velocity, algal cell deposition increased dramatically as the flux was increased above 50 lmh. For both crossflow velocities of 0.107 m/s and 0.175 m/s, transmembrane pressure data alone failed to detect these significant increases on the membrane surface. This is due to the limited ability of transmembrane pressure data to sense algal cell deposition on the membrane surface as initially it does not result in significant changes in overall permeability.

With data from image analysis of the membrane surface (shown in Fig. 6) it is evident that at 0.237 m/s the algal coverage was negligible. Therefore, it could be concluded that the deviation of transmembrane pressure from clean water values was due to other substances (EPS) within the feed solution, and not just the algal cells themselves. Further experiments were then carried out to explore these phenomena.

The algae used for further experiments was from a different batch, but was grown at the same conditions. Using data analysis, the pattern of behaviour of average transmembrane pressure iterated by flux stepping were very similar for each crossflow velocity. Similar trends were shown throughout for all the crossflow velocity values. At higher fluxes, the rate of increase of transmembrane pressure increased. The analysis

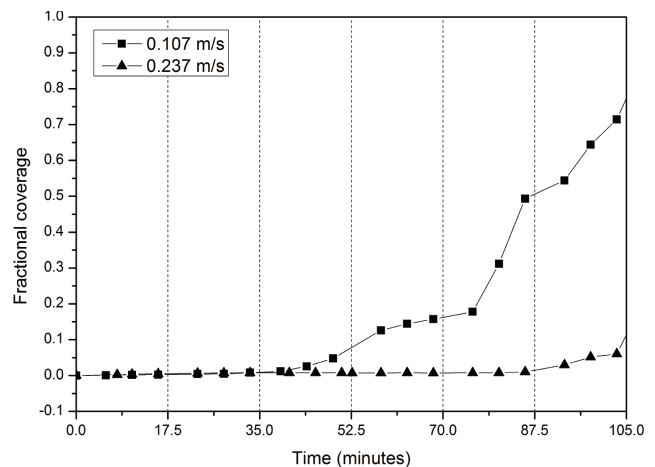


Fig. 6. Fractional membrane coverage by the algal cells against time for 29 mg/l algae solution at different crossflow velocities when flux stepping started from below the critical flux of the algal cells.

of organic content of both the permeate and the feed revealed a more intriguing observation which is the main focus of this paper.

3.1.2. Analysis of organic content

EPS-Polysaccharides (Carbohydrate content) EPS-Polysaccharide content of the feed remained relatively constant. The supernatants had values of around 2 ppm whilst the pellets had values in the range 6–8 ppm. EPS-protein was also measured throughout; however its concentration was negligible or was below the detection limit.

Fig. 7 shows permeate EPS vs flux at different crossflows. As crossflow velocity increased, the peak of polysaccharide content in the permeate shifts towards the left, from a flux of around 180 lmh to 116 lmh at crossflow velocity of 0.175 m/s and 0.237 m/s respectively. The peak value has also become more noticeable at crossflow velocity of 0.175 m/s and 0.237 m/s than at 0.107 m/s. This indicates that, during the flux stepping, as flux increases, greater amounts of EPS-polysaccharide were caused to penetrate through the membrane. There exists a flux at which the penetration of EPS is a maximum. After this flux, the concentration of EPS-polysaccharide in the permeate reduces. This could be due to fouling within the membrane pores by EPS.

EPS-polysaccharide concentration of the collected permeate eventually became higher than the concentration of EPS-Polysaccharide in the supernatant (feed solution), but it is still lower than EPS-Polysaccharide concentration extracted from the pellets. For the solution, this implies that $C_p > C_b$, which disagrees with the conventional filtration equation. Also the concentration

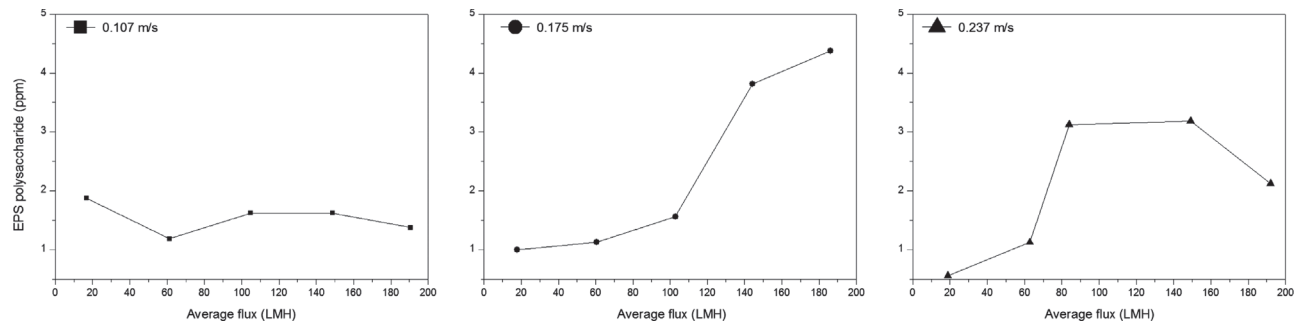


Fig. 7. EPS-Polysaccharide of the permeate at different crossflow velocities.

polarisation equation yields $C_w = (C_b - C_p) \cdot \exp(j/k) + C_p$, which implies lower concentration at the membrane surface as mass transfer coefficient increases as a result of higher crossflow velocity. In principle the sources of this extra amount of EPS-Polysaccharide in the permeate are: (i) the EPS of the supernatant of the feed solution accumulating on the membrane surface, or (ii) the EPS from the sheath surrounding the algal cells, or (iii) extra EPS released by the algal cells due to stress experienced at the membrane surface or some combination of these.

3.1.3. TOC and IC

Most feed concentrations had an inorganic carbon concentration of 0.15 ± 0.05 mg per mg of algae. For all conditions, Total Organic Carbon content of the permeate was much higher than that of the feed solution. A trend of transmission can be seen, nevertheless a clear explanation of the trend cannot be made.

Information from TOC content indicates that there is a possibility of retained carbon content on the membrane surface at the second flux stepping at all crossflow velocities. This retained carbon content could be EPS molecules resulting from accumulation of the cake on the membrane surface or within the membrane pore. It is hypothesized that as flux increased, local fluxes became high enough to disturb the retained solutes, resulting in more small solutes passing through the membrane pores; hence increased values would be detected in the permeate. As flux increased further, the resulting EPS-Polysaccharide and TOC content reduced. One possibility of this is that the membrane became more fouled as a result of accumulated solutes prior to that stepping. One possibility is that at this point, the flux is above the critical flux of the algal cells, and the fouling mechanism due to external pore blocking by the algal cells has started to take place.

3.2. Effect of membrane pore size

The trend of average transmembrane pressure against flux of filtration of algae at CFV of 0.107 m/s

using 0.1 μm and 0.2 μm Anopore membranes were very similar. However analysis of organic content revealed interesting differences as shown in Figs. 8 and 9.

With 0.1 μm , EPS-Polysaccharide concentration of the permeate at different fluxes was found to remain low, however it was slightly higher than the EPS concentration of the feed supernatant. The peak values of TOC remained at a flux of 100 lmh for both 0.1 μm and 0.2 μm . It can be seen clearly in Figs. 8 and 9 that both the EPS and TOC content in the permeate were much higher than that in the feed. Also this effect was much more pronounced at all fluxes for the 0.1 μm membrane, the smaller pore size membrane, than for the 0.2 μm membrane.

3.3. Effect of membrane type

For PVDF membranes, very similar transmembrane pressure trends to those of the Anopore membrane of

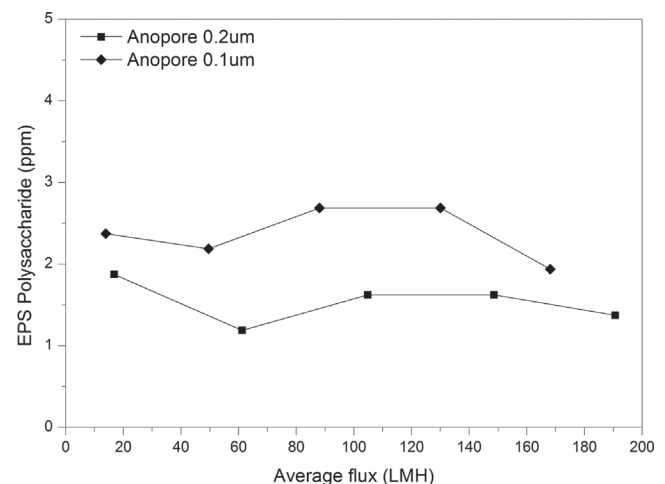


Fig. 8. Carbohydrate content or EPS (ppm) in the permeate from Anopore membranes with pore size 0.1 μm and 0.2 μm for algae solution at 29 mg/l at CFV of 0.107 m/s.

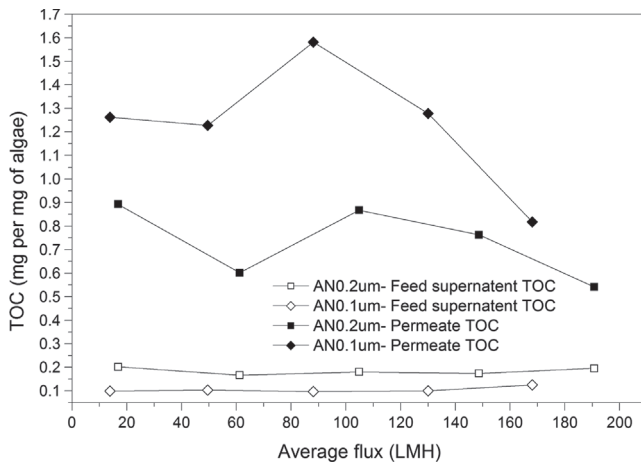


Fig. 9. Total organic carbon (mg per mg of algae) in the permeate and in the feed supernatant with Anopore membranes of pore size 0.1 μm and 0.2 μm. Operation at CFV of 0.107 m/s with algae solution at 29 mg/l.

the same pore size was found. However, PVDF, with its broader pore size distribution and interconnected pores, resulted in considerably more EPS and TOC transmission. The EPS-Polysaccharide transmission was high even at low fluxes, and the values are much higher than the EPS content of the feed. The trend of EPS-Polysaccharide concentration was similar to TOC content trend. Decreasing values of EPS-Polysaccharide and TOC concentration could imply that the membrane was fouled, therefore less of the organic particles could pass through. These results are illustrated by Figs. (10–12).

It was found that there is a possible relationship between the transition flux (defined as the flux at which a TMP jump occurs and sometimes defined by others as

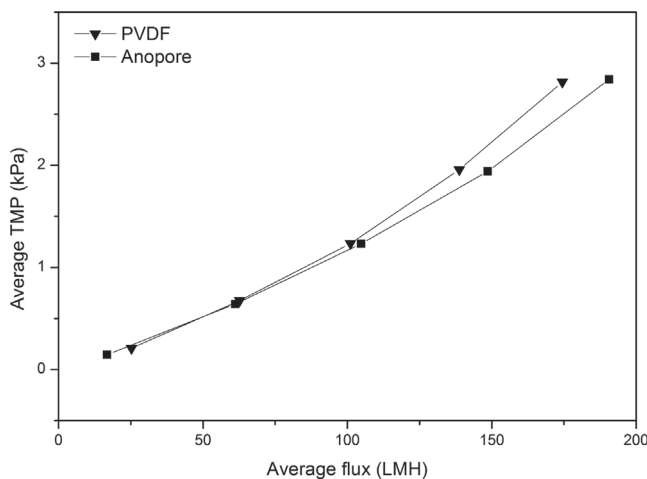


Fig. 10. Transmembrane pressure against flux for algae solution at 29 mg/l for Anopore and PVDF 0.2 μm membrane at CFV of 0.107 m/s.

the critical flux) and shear stress experienced by biopolymer molecules. When an EPS molecule is subject to high shear, the molecule elongates and its cross-sectional area is reduced. The stretched EPS molecules could then enter the membrane pores more easily. The expectation would be that at the same flux, EPS-content of the permeate would be greater at higher crossflow velocities and this was proven to be the case. Stretching of EPS molecules during crossflow filtration could also occur near the mouth of the pores where the change in fluid velocity is higher, and except at the highest fluxes, the EPS content

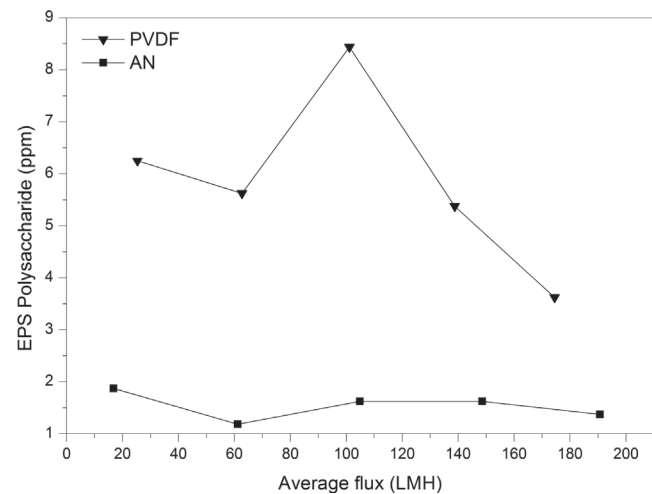


Fig. 11. EPS Polysaccharide in the permeate for Anopore and PVDF 0.2 μm membrane at CFV of 0.107 m/s.

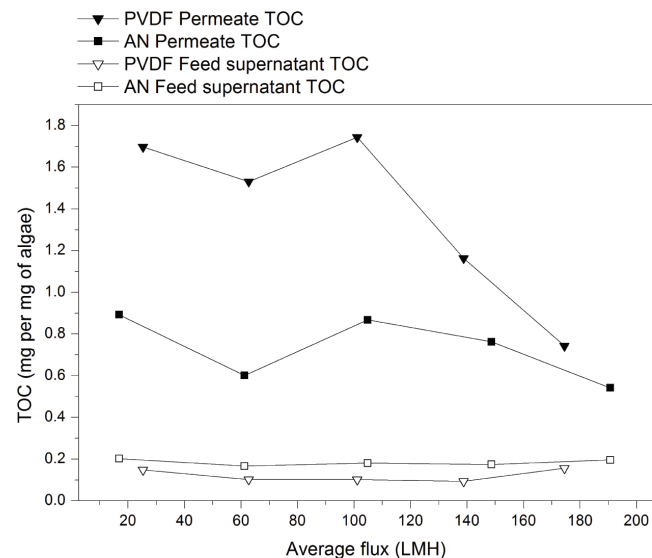


Fig. 12. Total organic carbon (mg per mg of algae) in the permeate (closed symbols) and in the feed supernatant (open symbols) with Anopore and PVDF 0.2 μm membranes. Operation at CFV of 0.107 m/s with algae concentration of 29 mg/l.

of the permeate does indeed increase with flux. From the review of a polymeric molecule transport through pore which will follow, one could conclude that upon entering the pore, a polymeric molecule is stretched and the conformation of the molecule within the pore depends not only on the pore diameter, but also the pore length and the length of the molecules. Along the pore length, there exists a pressure gradient which relates directly to the shape of viscoelastic molecules. With higher shear near the pore entrance and lower shear deeper in the pore, the molecule can more easily return from cigar-like conformation to a deformed conformation which can then cause internal pore fouling.

The transport of another flexible biopolymer, DNA, through filtration membranes has also been studied. Transmission of DNA was found to increase as DNA size decreases [20]. Elongation or deformation of DNA due to shear led to higher transmission at higher transmembrane pressure, and the DNA transmission was found to be highest for the smallest molecules [20–22]. Flux-dependent transmission of supercoiled plasmid DNA through ultrafiltration membranes has also been found [23]. With different nominal molecular weight cut-offs, the plasmid sieving coefficient “increased from zero to nearly one” as flux increases. Elongation of DNA, shear deformation, and concentration polarization were considered, “flow-induced elongation or deformation” was found to be crucial. However, in their studies, shear on the feed side, i.e., the stirring speed, was found not to influence DNA transmission. It is possible that the stirring in their system failed to provide sufficient energy for pre-deformation of the DNA molecules. Further studies are needed if a general conclusion is to be made.

Another mechanism that could be responsible for higher transmission of EPS at higher crossflow velocity could be the mechanically simulated hindered transport through the gel layer on the membrane surface, nevertheless, this mechanism alone cannot explain the flux dependent transport. Concentration polarisation leads to deposition of viscoelastic molecules on the membrane. The gel structure, which is not a uniform structure as local shear close to pores is higher than elsewhere, depends upon the hydrodynamic conditions of the system. Deposited EPS on the membrane surface can be viewed as a dynamic hydrogel with a structure which varies significantly with the micro environment. A polymeric gel consists of a solid network in a fluid phase. In the equilibrium state, hydrostatic forces and osmotic pressures (fluid phase forces) balance the elastic response of the polymer chains. When an equilibrium is disturbed, the polymeric network is deformed and the fluid is redistributed. This largely determines the macroscopic mechanical behaviour of these systems [24]. The transport of macromolecules within polymeric gels is

due to the dynamic equilibrium between matrix deformation, fluid pressure, and interstitial velocity, as well as the mechanical environment [24]. Mechanical deformation of a polymeric gel matrix can lead to the convective transport of macromolecules due to simple mechanical stimulation even without the presence of concentration gradients [24]. Periodic mechanical loading enhanced transport has also been found [25]. These studies were performed using relatively stable hydrogels whilst the present work involved a diluter system albeit one that may have a highly deformable dynamic gel layer next to a filtration surface. It has been reported that a membrane filtration model based on the viscosity dependency of the mass transfer coefficient which might well explain the sharp increase in TMP at higher fluxes but this does not offer an explanation for the changes in the permeate concentration [26].

3.4. Transport of a polymeric molecules

Many polymers are known for their shear thinning properties which could lead to higher transmission through the membrane at different shear stresses. A brief review on the transport of a polymeric molecules is presented here because this can be used to explain the shear dependent transmission of flexible molecules. The review starts by outlining the mechanism of a polymer chain entering the pore, being confined, then ejected.

In macromolecule studies, the mechanism of polymeric molecules entering a narrow channel has been studied. A polymer is known to change its conformation upon entering a narrow path. As a polymer becomes confined, its conformation changes. It starts by aligning its longest axis along the channel axis without much extension along the channel. This is followed by parallel expansion of polymer along the channel. Afterwards, the chain conformation within the channel changes to that of a random coil [27]. Upon entering the pore where the polymer's radius of gyration in bulk solution is equal or larger than the pore radius, then a portion of the chain is strongly stretched (known as stem), and the remaining rests just outside the pore (known as crown) [28]. This flower conformation occurs when the centre of mass is approximately one radius of gyration from the pore mouth. Once the centre of mass of the chain is positioned at twice the chain's radius of gyration inside the pore, the chain will change from flower conformation to a new conformation (deformed coil), see Fig. 13 [28]. During this process, there exists an immediate suction of the crown fraction into the pore when the chain reaches a certain distance into the pore [29]. In the case where adsorption of monomer onto the pore wall and the outer surface occurs, the crown is adsorbed on the surface and the stem becomes less stretched [28]. The

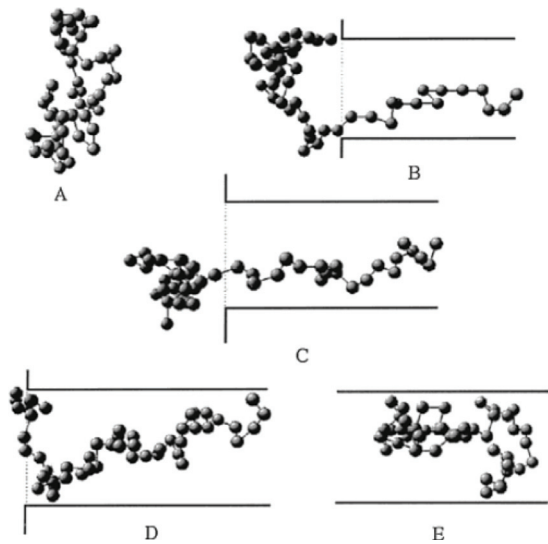


Fig. 13. “Snapshots of various degrees of polymer penetration ϕ : (A) bulk, (B) $\phi = 28\%$, (C) $\phi = 42\%$, (D) $\phi = 89\%$, (E) bulk pore”. Reproduced with permission [28].

results were not affected even with mild monomer-wall attractive interactions [28].

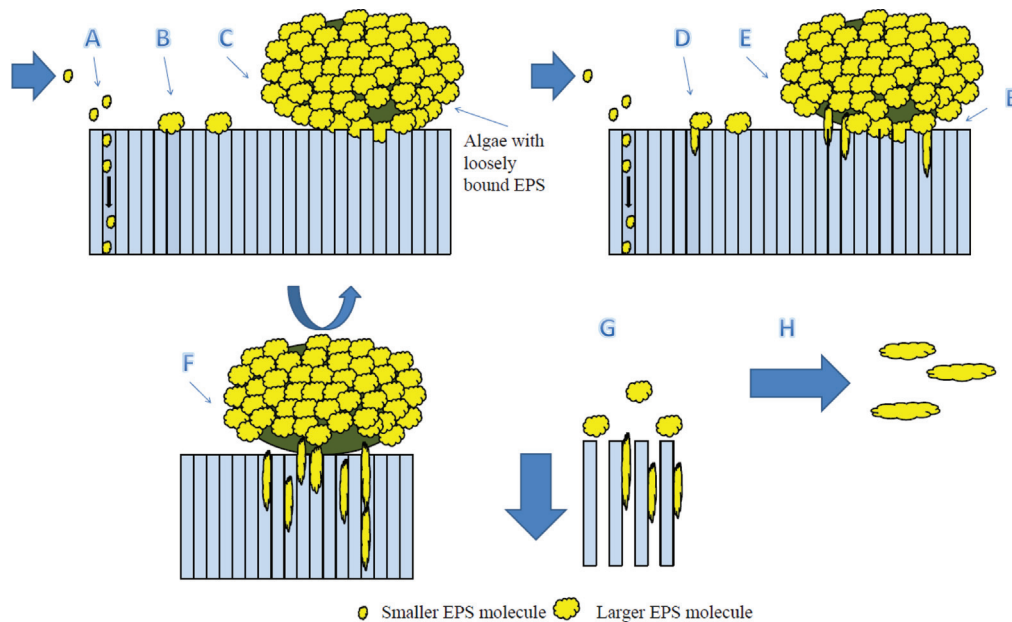
However, at sufficiently low concentrations in the solution exterior to the channel, the chains find it difficult to enter the channel. However at higher concentrations, the polymer characteristic length decreases in the exterior. When the characteristic length becomes smaller than the pore diameter; polymer chains will rush into the channel (weak-to-strong penetration transition) [27].

The transport of the molecules through the pore varies with not only its gyration radius, but also the pore diameter, pore length, and most importantly the relative length of polymer to the length of pore. In a confinement of two opposing walls of a piston, relation between the escape width and polymer length and piston radius has been found [28]. This is because the flower conformation plays an important part in the ejection of polymeric molecules from the pore. The behaviour of a polymer molecule within a pore is not well understood despite intensive research during the past decades [30]. The polymer residence time was found to increase and then decrease with molecular weight of the polymer, nevertheless above a threshold value, further increase in residence time was not observed [31]. It was concluded that when the polymer is relatively large in comparison to the pore size, “the out-of-the-pore part of the molecule pulls on the trapped part, thus acting as an entropic spring” [31]. The ejection kinetics of the case where the polymer is fully confined within the pore and partially confined with a fraction of a chain outside the pore are very different [30]. The simple diffusion of the molecules along the tube is responsible for the former.

Flow in microfluidic devices especially those involving extension are considered to be different to those in macroscale channels [32]. The effect of elastic properties even in low viscosity aqueous polymer solution (2–3 mPas) has been seen in high speed processes [32]. Unstable streamlines along the depth of the channel containing 0.1–0.5% PAA in water have been visualised [32]. In flow visualisation of low concentration PEO through polydimethylsiloxane (PDMS), sharp features at the contraction entrance, coupled with the fluid elasticity leads to growth of vortices upstream, and suppression of those downstream [32]. Deposition of PEO material was observed on the surface near the contraction throat. The deposited material was asymmetric and led to asymmetric flow [32]. The suppression of downstream vortices could be due to kinetic energy being absorbed by the polymer molecules during their deformation along the channel length. This is supported by observations on pressure drop. As polymer chains reach their finite extensibility limit, further pressure drop was not observed, and polymer chains act as a highly anisotropic viscous fluid [32]. The hindrance effect of polymer mobility by chain-chain interaction can be present at high concentrations [32]. At higher polymer concentrations, the critical deformation rate becomes lower and the magnitude of the increase in the extensional viscosity increases [33].

3.5. Rationalisation of visual observation of algae deposition and removal on membrane surface

With the use of DOTM, deposition and removal mechanism of algal cells can be visually observed. A schematic picture describing a possible transport of EPS through the membrane is shown in Fig. 14. Now consider when the algal cells, surrounded by its EPS sheath, come into contact with the membrane surface. If the tangential shear exceeds the adhesion force (EPS-membrane adhesion force), then the algae will be lifted away from the membrane surface. If the tangential shear is less than the adhesion force, the algae will stick to the membrane until tangential shear exceeds the EPS molecule-molecule linkage force causing tearing of the sheath. The algae will then be released from the sheath and rolled out. Also if the local flux, especially the local flux near to the deposited algae is higher than critical shear of the EPS, then the EPS will be deformed and pass through the pores leaving the algae with a reduced adhesion force to the membrane. After this, whether the algal cell will get stuck to a neighbouring part of the membrane surface depends on the remaining amount of EPS in the surrounding algal cells. If the algal cell is still surrounded by a sufficient amount of remaining sheath, the algae removal process will repeat until the tangential shear



- (A) The smaller size EPS can permeate through the pores freely, however a portion of these are attached to the membrane pores.
 (B) The larger size EPS comes into contact with the membrane surface and contributes to higher membrane resistance.
 (C) An algal cell comes into close contact with the membrane surface, the adhesion of the sheath causes the algal cell to attach to the membrane.
 (D) Some of the larger size EPS that comes into contact with the membrane surface starts to elongate due to the higher local shear experienced.
 (E) Similar phenomenon is also experienced by the sheath.
 (F) For algae removal, parts of the attached EPS elongated and is able to pass through the pores. This reduces adhesion force. When shear is higher than adhesion force, the algal cell then rolls to the side causing other EPS to attach to the next available surface. This repeats until the effect of shear is higher than adhesion force, or the algal cell is removed from its sheath by shear.
 (G) At higher flux, local extensional flow is higher, hence higher amount of larger EPS are elongated. More become able to pass through the pores. For smaller pore size, the extensional flow is higher than in the larger pore resulting in higher EPS permeation at the same flux.
 (H) At higher crossflow velocity, larger EPS is already partly elongated, enabling higher transmission through the membrane pores at lower local flux.

Fig. 14. Interaction of algae and EPS with membrane: Physical model to rationalise observation.

exceeds the adhesion force or lead to the release of the cell from its sheath. Nevertheless, further observations, and testing of permeate must be carried out to confirm this hypothesis.

In the case where the algae have aged, and when salt concentration of the feed was altered, especially with CaCl₂ addition, agglomeration of the EPS around the algae occurred. It was visible through a microscope that the EPS deposition on the membranes became thicker and larger. The EPS were visually observed to be more abundant and tear less easily, leading to lower algal removal from the membrane surface as well as thicker formation of the algal cell layer on the membrane surface. It was also found that lowering concentration of the algae is not always beneficial.

Many MBRs have been studied and one of the interesting findings is that fouling resistance is caused by mostly loosely bound EPS rather than tightly bound EPS [8]. Although it has been observed that tightly bound EPS is responsible for high filtration resistance,

the filtration resistance in mixed suspension is controlled by loosely bound EPS fraction [34]. This fits well with our rationalisation.

It has been suggested in discussion with others that higher fluxes increase concentration polarisation and that this is the cause of higher transmission. Whilst for a fixed intrinsic separation factor this is true, the key observation that we have sought to explain is the increase in transmission at high crossflow velocities as compared to that at lower crossflow velocities. Focusing upon concentration polarisation does not explain this; indeed increases in crossflow velocity will lead to a decreased concentration polarisation adjacent to the surface.

4. Conclusion

Experiments has been carried out on the filtration of *Chlorella Sorokiniana*. The results showed that transport of EPS through microfiltration membranes is affected by both the permeate flux and the crossflow velocity.

Unlike many previous results for other macromolecules, increased crossflow velocity resulted in higher transmission of EPS at the same flux, as well as a higher rate of increase of transmembrane pressure. Several mechanisms have been considered and a rationalisation of observations has been made. There is a possibility that for filtration of biopolymers or similar feed molecules, fouling can be linked to a macromolecule's critical shear. Rheological properties of a sample feed could be examined in order to calculate the most suitable filtration conditions for the feed.

Acknowledgements

Some of this work was carried out at the Singapore Membrane Technology Centre (SMTC). The SMTC is grateful for support from the Singapore Economic Development Board (EDB) and the Environment and Water Industry Council (EWI). Dr. A. Lubansky is also thanked for his help with this manuscript.

References

- [1] Boksoon Kwon, Noeon Park and Jaeweon Cho, Effect of algae on fouling and efficiency of UF membranes, *Desalination, Membranes in Drinking and Industrial Water Production*, 179(1–3) (2005) 203–214.
- [2] D.R. Vardon, M.M. Clark and D.A. Ladner, Effects of shear on microfiltration and ultrafiltration fouling by marine bloom-forming algae, *J. Membr. Sci.*, 356(1–2) (2010) 33–43, cited by (since 1996).
- [3] B. Petrushevski, G. Bolier, A.N. Van Breemen and, G.J. Alaerts, Tangential flow filtration: A method to concentrate freshwater algae, *Water Res.*, 29(5) (1995) 1419–1424.
- [4] Masato Imase, Keiji Watanabe, Hideki Aoyagi and Hideo Tanaka, Construction of an artificial symbiotic community using a chlorella-symbiont association as a model, *FEMS Microbiol. Ecol.*, 63(3) (2008) 273–282.
- [5] Gary G. Leppard, The characterization of algal and microbial mucilages and their aggregates in aquatic ecosystems, *Sci. Total Environ.*, 165(1–3) (1995) 103–131.
- [6] K. Watanabe, M. Imase, K. Sasaki, N. Ohmura, H. Saiki and H. Tanaka, Composition of the sheath produced by the green algae *Chlorella sorokiniana*, *Lett. Appl. Microbiol.*, 42(5) (2006) 538–543.
- [7] Keiji Watanabe, Noritaka Takihana, Hideki Aoyagi, Satoshi Hanada, Yoshitomo Watanabe, Naoya Oh-mura, Hiroshi Saiki and Hideo Tanaka, Symbiotic association in chlorella culture, *FEMS Microbiol. Ecol.*, 51(2) (2005) 187–196.
- [8] F. Meng, S.-R. Chae, A. Drews, M. Kraume, H.-S. Shin and F. Yang, Recent advances in membrane bioreactors (mbrs): Membrane fouling and membrane material, *Water Res.*, 43(6) (2009) 1489–1512.
- [9] Sandhya Babel, Satoshi Takizawa and Hiroaki Ozaki, Factors affecting seasonal variation of membrane filtration resistance caused by chlorella algae, *Water Res.*, 36(5) (2002) 1193–1202.
- [10] S. Babel and S. Takizawa, Microfiltration membrane fouling and cake behavior during algal filtration, *Desalination*, 261(1–2) (2010) 46–51.
- [11] Y.-T. Chiou, M.-L. Hsieh and H.-H. Yeh, Effect of algal extracellular polymer substances on UF membrane fouling, *Desalination*, 250(2) (2010) 648–652.
- [12] M.T. Hung and J.C. Liu, Microfiltration for separation of green algae from water, *Colloids Surf., B*, 51(2) (2006) 157–164.
- [13] Antoine Montiel and Bénédicte Welté, Preozonation coupled with flotation filtration: Successful removal of algae, *Water Sci. Technol.*, 37(2) (1998) 65–73, Reservoir Management and Water Supply—An Integrated System, Selected Proceedings of the First IAWQ-IWSA Joint Specialist Conference on Reservoir Management and Water Supply—An Integrated System.
- [14] J. Wang, J. Guan, S.R. Santiwong and T. David Waite, Characterization of floc size and structure under different monomer and polymer coagulants on microfiltration membrane fouling, *J. Membr. Sci.*, 321(2) (2008) 132–138.
- [15] H. Li, A.G. Fane, H.G.L. Coster and S. Vigneswaran, Direct observation of particle deposition on the membrane surface during crossflow microfiltration, *J. Membr. Sci.*, 149(1) (1998) 83–97.
- [16] Whatman. <http://www.whatman.com/>, Retrieved 2009.
- [17] www.2spi.com.
- [18] F. Wicaksana, P. Pongpairaj, R.W. Field, Z.F. Cui and A.G. Fane, Critical flux determination of microalgae (*Chlorella sorokiniana*) filtration using direct observation through the membrane (DOTM) technique, In preparation for *J. Membr. Sci.*
- [19] <http://www.originlab.com/>.
- [20] T. Hirasaki, T. Sato, T. Tsuboi, H. Nakano, T. Noda, A. Kono, K. Yamaguchi, K. Imada, N. Yamamoto, H. Murakami and S. Manabe, Permeation mechanism of dna molecules in solution through cuprammonium regenerated cellulose hollow fiber, *J. Membr. Sci.*, 106(1–2) (1995) 123–129.
- [21] D.W. Kahn, M.D. Butler, D.L. Cohen, M. Gordon, J.W. Kahn and M.E. Winkler, Purification of plasmid dna by tangential flow filtration, *Biotechnol. Bioeng.*, 69(1) (2000) 101–106.
- [22] S. Kong, N. Titchener-Hooker and M.S. Levy, Plasmid DNA processing for gene therapy and vaccination: Studies on the membrane sterilisation filtration step, *J. Membr. Sci.*, 280(1–2) (2006) 824–831.
- [23] D.R. Latulippe, K. Ager and A.L. Zydney, Flux-dependent transmission of supercoiled plasmid dna through ultrafiltration membranes, *J. Membr. Sci.*, 294(1–2) (2007) 169–177.
- [24] P.A. Netti, F. Travascio and R.K. Jain, Coupled macromolecular transport and gel mechanics: Poroviscoelastic approach, *AIChE J.*, 49(6) (2003) 1580–1596.
- [25] K.Y. Lee, M.C. Peters, K.W. Anderson and D.J. Mooney, Controlled growth factor release from synthetic extracellular matrices, *Nature*, 408(6815) (2000) 998–1000.
- [26] P. Aimar and R.W. Field, Limiting flux in membrane separations: A model based on the viscosity dependency of the mass transfer coefficient, *Chem. Eng. Sci.*, 47(3) (1992) 579–586.
- [27] I. Teraoka and Y. Wang, Computer simulation studies on overlapping polymer chains confined in narrow channels, *Polymer*, 45(11) (2004) 3835–3843.
- [28] G.F. Hermsen, B.A. De Geeter, N.F.A. Van der Vegt and M. Wessling, Monte carlo simulation of partially confined flexible polymers, *Macromolecules*, 35(13) (2002) 5267–5272.
- [29] L.I. Klushin, A.M. Skvortsov, H.-P. Hsu and K. Binder, Dragging a polymer chain into a nanotube and subsequent release, *Macromolecules*, 41(15) (2008) 5890–5898.
- [30] A. Milchev, L. Klushin, A. Skvortsov and K. Binder, Ejection of a polymer chain from a nanopore: Theory and computer experiment, *Macromolecules*, 43(16) (2010) 6877–6885.
- [31] O.V. Krasilnikov, C.G. Rodrigues and S.M. Bezrukov, Single polymer molecules in a protein nanopore in the limit of a strong polymer-pore attraction, *Phys. Rev. Lett.*, 97(1), 2006.
- [32] L.E. Rodd, T.P. Scott, D.V. Boger, J.J. Cooper-White and G.H.c McKinley, The inertio-elastic planar entry flow of low-viscosity elastic fluids in micro-fabricated geometries, *J. Non-Newtonian Fluid Mech.*, 129(1) (2005) 1–22.
- [33] G.H. McKinley, L.E. Rodd, M.S.N. Oliverira and J. Cooper-White, Extensional flows of polymer solutions in microfluidic converging/diverging geometries, *Journal of Central South University of Technology (English Edition)*, 14(1 SUPPL.) (2007) 6–9.
- [34] A. Ramesh, D.J. Lee and J.Y. Lai, Membrane biofouling by extracellular polymeric substances or soluble microbial products from membrane bioreactor sludge, *Appl. Microbiol. Biotechnol.*, 74(3) (2007) 699–707.